

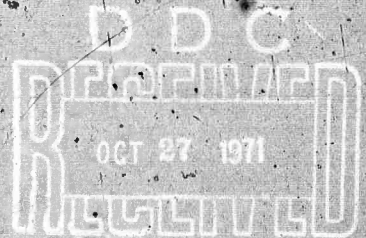
THE HYPERSONIC LEADING EDGE PROBLEM
II. WEDGES AND CONES

Michael L. Shorenstein

April 1971

FLUID MECHANICS LABORATORY

Reproduced by
**NATIONAL TECHNICAL
INFORMATION SERVICE**
Springfield, Va. 22151



DEPARTMENT OF MECHANICAL ENGINEERING
MASSACHUSETTS INSTITUTE OF TECHNOLOGY

47

DOCUMENT CONTROL DATA - R&D

(Security classification of title, body of abstract and indexing annotation must be entered when the overall report is classified)

1. ORIGINATING ACTIVITY (Corporate author) Massachusetts Institute of Technology Cambridge, Massachusetts 02139		2a. REPORT SECURITY CLASSIFICATION Unclassified	
		2b. GROUP	
3. REPORT TITLE THE HYPERSONIC LEADING EDGE PROBLEM II. WEDGES AND CONES			
4. DESCRIPTIVE NOTES (Type of report and inclusive dates)			
5. AUTHOR(S) (Last name, first name, initial) Shorenstein, Michael L.			
6. REPORT DATE April 1971		7a. TOTAL NO. OF PAGES 42	7b. NO. OF REFS 19
8a. CONTRACT OR GRANT NO. N00014-0204-0040		9a. ORIGINATOR'S REPORT NUMBER(S) Fluid Mechanics Laboratory Publication No. 71-9	
b. PROJECT NO.		9b. OTHER REPORT NO(S) (Any other numbers that may be assigned this report)	
c.			
d.			
10. AVAILABILITY/LIMITATION NOTICES Distribution unlimited			
11. SUPPLEMENTARY NOTES		12. SPONSORING MILITARY ACTIVITY Advanced Research Projects Agency, Department of Defense and Office of Naval Research, Washington, D.C.	
13. ABSTRACT An analysis is given for the viscous hypersonic flow past slender sharp wedges and unyawed cones. The leading edge or nose region treated encompasses the merged layer regime in which the shock thickness is not small in comparison with the viscous layer thickness but for which in the axisymmetric case the shock thickness is small in comparison with the radius of transverse shock curvature. A Navier-Stokes flow is assumed, and both the shock structure and viscous layer are taken to be locally-similar of boundary layer type. The analysis follows that used by Shorenstein and Probstain for the corresponding flat plate problem. For axisymmetric cone flow, a modification of a transformation introduced by Probstain and Elliott is given to reduce the axisymmetric viscous layer equations including transverse curvature to "exactly" two-dimensional form. Results for the state conditions behind the shock, and the wall pressure, skin friction, and heat transfer rate are found to be in good agreement with available experimental data.			

Security Classification

14. KEY WORDS	LINK A		LINK B		LINK C	
	ROLE	WT	ROLE	WT	ROLE	WT
Hypersonic flow						
Sharp leading edge						
Merged layer regime						
Wedges and cones						

INSTRUCTIONS

1. **ORIGINATING ACTIVITY:** Enter the name and address of the contractor, subcontractor, grantee, Department of Defense activity or other organization (corporate author) issuing the report.
- 2a. **REPORT SECURITY CLASSIFICATION:** Enter the overall security classification of the report. Indicate whether "Restricted Data" is included. Marking is to be in accordance with appropriate security regulations.
- 2b. **GROUP:** Automatic downgrading is specified in DoD Directive 5200.10 and Armed Forces Industrial Manual. Enter the group number. Also, when applicable, show that optional markings have been used for Group 3 and Group 4 as authorized.
3. **REPORT TITLE:** Enter the complete report title in all capital letters. Titles in all cases should be unclassified. If a meaningful title cannot be selected without classification, show title classification in all capitals in parenthesis immediately following the title.
4. **DESCRIPTIVE NOTES:** If appropriate, enter the type of report, e.g., interim, progress, summary, annual, or final. Give the inclusive dates when a specific reporting period is covered.
5. **AUTHOR(S):** Enter the name(s) of author(s) as shown on or in the report. Enter last name, first name, middle initial. If military, show rank and branch of service. The name of the principal author is an absolute minimum requirement.
6. **REPORT DATE:** Enter the date of the report as day, month, year, or month, year. If more than one date appears on the report, use date of publication.
- 7a. **TOTAL NUMBER OF PAGES:** The total page count should follow normal pagination procedure, i.e., enter the number of pages containing information.
- 7b. **NUMBER OF REFERENCES:** Enter the total number of references cited in the report.
- 8a. **CONTRACT OR GRANT NUMBER:** If appropriate, enter the applicable number of the contract or grant under which the report was written.
- 8b, 8c, & 8d. **PROJECT NUMBER:** Enter the appropriate military department identification, such as project number, subproject number, system numbers, task number, etc.
- 9a. **ORIGINATOR'S REPORT NUMBER(S):** Enter the official report number by which the document will be identified and controlled by the originating activity. This number must be unique to this report.
- 9b. **OTHER REPORT NUMBER(S):** If the report has been assigned any other report numbers (either by the originator or by the sponsor), also enter this number(s).
10. **AVAILABILITY/LIMITATION NOTICES:** Enter any limitations on further dissemination of the report, other than those

imposed by security classification, using standard statements such as:

- (1) "Qualified requesters may obtain copies of this report from DDC."
- (2) "Foreign announcement and dissemination of this report by DDC is not authorized."
- (3) "U. S. Government agencies may obtain copies of this report directly from DDC. Other qualified DDC users shall request through _____."
- (4) "U. S. military agencies may obtain copies of this report directly from DDC. Other qualified users shall request through _____."
- (5) "All distribution of this report is controlled. Qualified DDC users shall request through _____."

If the report has been furnished to the Office of Technical Services, Department of Commerce, for sale to the public, indicate this fact and enter the price, if known.

11. **SUPPLEMENTARY NOTES:** Use for additional explanatory notes.
12. **SPONSORING MILITARY ACTIVITY:** Enter the name of the departmental project office or laboratory sponsoring (paying for) the research and development. Include address.
13. **ABSTRACT:** Enter an abstract giving a brief and factual summary of the document indicative of the report, even though it may also appear elsewhere in the body of the technical report. If additional space is required, a continuation sheet shall be attached.

It is highly desirable that the abstract of classified reports or short phrases that characterize a report and may be used as an indication of the military security classification of the information in the paragraph, represented as (TS), (S), (C), or (U).

There is no limitation on the length of the abstract. However, the suggested length is from 150 to 225 words.

14. **KEY WORDS:** Key words are technically meaningful terms or short phrases that characterize a report and may be used as index entries for cataloging the report. Key words must be selected so that no security classification is required. Identifiers, such as equipment model designation, trade name, military project code name, geographic location, may be used as key words but will be followed by an indication of technical context. The assignment of links, rules, and weights is optional.

THE HYPERSONIC LEADING EDGE PROBLEM

II. WEDGES AND CONES

by

Michael L. Shorenstein

Fluid Mechanics Laboratory

**Department of Mechanical Engineering
Massachusetts Institute of Technology**

This work was supported by the Advanced Research Projects Agency of the Department of Defense and was monitored by the Office of Naval Research under Contract No. N00014-0204-0040, ARPA Order No. 322.

This document has been approved for public release and sale; its distribution is unlimited.

April 1971

THE HYPERSONIC LEADING EDGE PROBLEM

II. WEDGES AND CONES

by

Michael L. Shorenstein*

Abstract

An analysis is given for the viscous hypersonic flow past slender sharp wedges and unyawed cones. The leading edge or nose region treated encompasses the merged layer regime in which the shock thickness is not small in comparison with the viscous layer thickness but for which in the axisymmetric case the shock thickness is small in comparison with the radius of transverse shock curvature. A Navier-Stokes flow is assumed, and both the shock structure and viscous layer are taken to be locally-similar of boundary layer type. The analysis follows that used by Shorenstein and Probstein for the corresponding flat plate problem. For axisymmetric cone flow, a modification of a transformation introduced by Probstein and Elliott is given to reduce the axisymmetric viscous layer equations including transverse curvature to "exactly" two-dimensional form. Results for the state conditions behind the shock, and the wall pressure, skin friction, and heat transfer rate are found to be in good agreement with available experimental data.

* The author wishes to thank sincerely Professor Ronald F. Probstein of M.I.T. for his support during the course of this investigation and for his valuable suggestions and criticisms. This research was supported by the Advanced Research Projects Agency and was technically administered by the Office of Naval Research under Contract No. N00014-0204-0040, ARPA Order No. 322.

Research Assistant, M.I.T., presently at Northern Research & Engineering Corp., Cambridge, Mass.

Nomenclature

A	= velocity ratio, u_s^*/U_∞
B	= given by Eq. (18)
C	= Chapman-Rubesin constant
C_1	= given by Eq. (20a)
C_2	= given by Eq. (20b)
c_F	= skin friction coefficient
c_p	= specific heat at constant pressure
D	= reduced density, ρ/ρ_∞
f	= streamfunction given by Eq. (6)
$(f_\eta)_b$	= reduced slip velocity, u_{sl}^*/u_s^*
F	= given by Eq. (43)
g	= shear stress, $Nf_{\eta\eta}$
$g(0)$	= value of g at body surface
h	= specific enthalpy, $c_p T$
H	= total enthalpy
I	= given by Eq. (11)
j	= index taken to be zero for two-dimensional flow and unity for axisymmetric flow
L	= arbitrary fixed reference length
M_∞	= freestream Mach number
n	= normal coordinate for shock structure
N	= given by Eq. (5)
p	= static pressure

P	= reduced pressure, $p/\rho_\infty U_\infty^2$
Pr	= Prandtl number
$Q_1(j)$	= given by Eq. (28)
$Q_2(j)$	= given by Eq. (29)
$Q_3(j)$	= given by Eq. (42)
r	= radius of transverse curvature, $r_b + y^* \cos \theta_b$
R	= gas constant
$Re_{x^*,\infty}$	= local Reynolds number, $\rho_\infty U_\infty x^*/\mu_\infty$
St	= Stanton number
T	= static temperature
T_0	= freestream stagnation temperature
u, u^*	= velocity component parallel to shock surface and to body surface, respectively [see Fig. 2]
U_∞	= freestream velocity
v, v^*	= velocity component normal to shock surface and to body surface, respectively [see Fig. 2]
\bar{v}	= transformed normal velocity given by Eq. (2a)
V	= reduced velocity, v/U_∞
W	= reduced velocity, u/U_∞
x^*, y^*	= coordinate along body surface and normal to body surface, respectively [see Fig. 2]
\bar{x}, \bar{y}	= transformed coordinates given by Eq. (2a)
α	= inverse Reynolds number $(\rho_\infty U_\infty r_b / \mu_\infty)^{-1}$
γ	= specific heat ratio
Δ_s	= shock thickness
ζ	= stretched normal coordinate for shock structure, Eq. (23)
η	= stretched normal coordinate for viscous layer, Eq. (6)

- η_b = transformed location of the body surface for the case of slip
- η_s = location of the shock surface
- θ_b = body surface inclination angle with respect to the free stream
- θ_s = shock surface inclination angle with respect to the body surface
- (H) = reduced enthalpy given by Eq. (6)
- μ = viscosity
- $\bar{\mu}$ = given by transformation Eq. (2b)
- ξ = transformed coordinate along body surface given by Eq. (6)
- ρ = density
- $\sigma(j)$ = cross-section of streamtube incident to viscous layer
- ϕ = reduced enthalpy given by Eq. (23)
- χ_∞ = interaction parameter, $M_\infty^3 (C/Re_{x^*, \infty})^{1/2}$

Subscripts

- b = condition at the body surface
- ns ℓ = quantity obtained from no-slip solution
- s = condition at the shock surface
- sl = quantity obtained from slip solution
- η = derivative with respect to η
- ∞ = condition at the freestream

I. Introduction

Two classes of continuum flow models have been investigated recently for treating the hypersonic flow past sharp bodies upstream of the strong interaction regime in the merged layer [see Fig. 1] where the shock thickness must be considered finite in comparison with the viscous layer thickness. One class¹⁻³ applies the full Navier-Stokes equations in finite difference form in order to determine to what extent a continuum may meaningfully describe the flow field in the merged layer. This complex scheme requires rather large computer storage space.

Another class of merged layer models⁴⁻⁶ uses the Navier-Stokes equations but assumes "local similarity" to apply in both the viscous layer and shock wave, that is, streamwise variations of all properties are taken to be sufficiently small, so that the Navier-Stokes equations, when applied locally, can be approximated by ordinary differential equations. This description of the merged viscous shock layer is obtained from locally-similar solutions "patched" at the interface between the outer shock structure portion and the inner viscous layer portion in which the equations are taken to be of boundary layer type with normal pressure gradient effects neglected. Results in Ref. 6 from such a merged layer model for a flat plate have compared well with experimental data⁷⁻⁹. The theoretical calculations have shown the relative importance of several rarefaction effects over a cold sharp flat plate aligned

parallel to the hypersonic freestream. Dominant among these effects was shown to be the finite shear at the interface between the back of the shock and the outer edge of the viscous layer. The effect of including velocity slip and temperature jump at the body surface was shown to be smaller but non-negligible, while the effect of including longitudinal shock curvature was found in comparison to be negligible.

The present analysis extends this flat plate continuum merged layer model of Ref. 6 to wedge and axisymmetric conical flows by investigating the additional effects of body slope and, for conical flow, the effects of axial symmetry and transverse curvature effects. Longitudinal shock curvature effects are neglected as small based on the results of Ref. 6. Body slope effects are characterized by the parameter θ_b , where θ_b is the half angle of the wedge or unyawed cone. The analysis is extended only to slender bodies with $\theta_b \ll 1$ for which the normal component of the viscous layer velocity can be neglected compared to the tangential component. This restriction is introduced in order to solve the viscous layer problem by the method of Ref. 6.

In the axial symmetric case, a modification of a Mangler type transformation given by Probstein and Elliott¹⁰ is introduced to reduce the axisymmetric viscous layer equations to an "exactly" two-dimensional form. The modification involves a transformation applied to the viscosity coefficient, and this transformation is shown to include the effects of transverse curvature characterized by the

parameter $M_\infty \alpha$. Here α is an inverse Reynolds number based on the body radius r_b of transverse curvature, and M_∞ is the freestream Mach number. A new term proportional to $M_\infty \alpha$ is found to modify the reduced viscous layer momentum equation of Ref. 6 and is shown to account for transverse curvature effects.

For the present investigation, two regimes of $M_\infty \alpha$ are distinguished: I, a regime immediately adjacent to the sharp nose where $M_\infty \alpha \gtrsim 1$ and II, a regime downstream of the sharp nose where $M_\infty \alpha \ll 1$. Only the second regime is treated here. This restriction is introduced to obtain a simple closed form shock structure solution by a method analogous to Ref. 6. In the conical shock structure equations, transverse shock curvature terms are of order Δ_s/r_s where Δ_s is the shock thickness and r_s is the radius of transverse shock curvature. It is found that if $M_\infty \alpha \ll 1$, then terms of order Δ_s/r_s are negligible compared to the other terms in the shock structure equations. These equations can then be reduced to the form of the "zero-order" shock equations solved in Ref. 6.

II. Viscous Layer

As in Ref. 6, the merged shock layer is described by a viscous layer of boundary layer type patched at an outer interface (the "shock surface") to a thick shock structure. The velocity and state variables from the solution of the viscous layer equations are matched locally at the shock surface to the corresponding quantities from the solution of the shock structure equations.

The governing equations for the viscous layer written in the local body-centered coordinate frame (x^*, y^*) depicted in Fig. 2 are

$$\frac{\partial}{\partial x^*} (r^j \rho u^*) + \frac{\partial}{\partial y^*} (r^j \rho v^*) = 0 \quad (1a)$$

$$\rho (u^* \frac{\partial u^*}{\partial x^*} + v^* \frac{\partial u^*}{\partial y^*}) = - \frac{dp}{dx^*} + \frac{\partial}{\partial y^*} (\mu \frac{\partial u^*}{\partial y^*}) + j \frac{\mu}{r} \frac{\partial r}{\partial y^*} \frac{\partial u^*}{\partial y^*} \quad (1b)$$

$$\begin{aligned} \rho (u^* \frac{\partial h}{\partial x^*} + v^* \frac{\partial h}{\partial y^*}) &= u^* \frac{dp}{dx^*} + \frac{1}{Pr} [\frac{\partial}{\partial y^*} (\mu \frac{\partial h}{\partial y^*}) \\ &+ j \frac{\mu}{r} \frac{\partial r}{\partial y^*} \frac{\partial h}{\partial y^*}] + \mu (\frac{\partial u^*}{\partial y^*})^2 \end{aligned} \quad (1c)$$

where $j = 0$ for two-dimensional flow and $j = 1$ for axisymmetric flow, with $r(x^*, y^*) = r_b(x^*) + y^* \cos \theta_b$ the local radius of transverse curvature for the case of axisymmetric flow with θ_b the body slope relative to the freestream direction. The tangential and normal components of velocity are u^* and v^* , respectively [see Fig. 2], h is the specific enthalpy, p is the pressure, μ is the viscosity, and Pr is the Prandtl number taken to be a constant.

Probstein and Elliott¹⁰ introduced a generalized Mangler transformation which reduced Eqs. (1) to an almost two-dimensional form by applying the transformations

$$\begin{aligned} d\bar{x} &= (\frac{r_b}{L})^{2j} dx^* \quad , \quad \frac{\partial}{\partial x^*} = (\frac{r_b}{L})^{2j} \frac{\partial}{\partial \bar{x}} + j (\frac{\partial \bar{y}}{\partial x^*}) \frac{\partial}{\partial \bar{y}} \\ d\bar{y} &= (\frac{r}{L})^j dy^* \quad , \quad \frac{\partial}{\partial y^*} = (\frac{r}{L})^j \frac{\partial}{\partial \bar{y}} \\ \bar{v} &= (\frac{rL}{r_b^2})^j v^* + j [(\frac{L}{r_b})^2 \frac{\partial \bar{y}}{\partial x^*}] u^* \end{aligned} \quad (2a)$$

where L is an arbitrary fixed reference length. By also introducing the transformation

$$\bar{\mu} = \left(1 + \frac{2jL \bar{y} \cos \theta_b}{r_b^2}\right) \mu \quad (2b)$$

Eqs. (1) can be reduced "exactly" to two-dimensional form. This follows from the fact that θ_b and r_b are functions of \bar{x} only, so that Eqs. (1) when transformed by means of Eqs. (2) give the homogeneous system

$$\frac{\partial}{\partial \bar{x}} (\rho u^*) + \frac{\partial}{\partial \bar{y}} (\rho \bar{v}) = 0 \quad (3a)$$

$$\rho \left(u^* \frac{\partial u^*}{\partial \bar{x}} + \bar{v} \frac{\partial u^*}{\partial \bar{y}} \right) - \frac{\partial}{\partial \bar{y}} \left(\bar{\mu} \frac{\partial u^*}{\partial \bar{y}} \right) + \frac{dp}{d\bar{x}} = 0 \quad (3b)$$

$$\rho \left(u^* \frac{\partial h}{\partial \bar{x}} + \bar{v} \frac{\partial h}{\partial \bar{y}} \right) - \frac{1}{Pr} \frac{\partial}{\partial \bar{y}} \left(\bar{\mu} \frac{\partial h}{\partial \bar{y}} \right) - \bar{\mu} \left(\frac{\partial u^*}{\partial \bar{y}} \right)^2 - u^* \frac{dp}{d\bar{x}} = 0 \quad (3c)$$

which are "two-dimensional" in form. It must be pointed out, however, that the parameter $\bar{\mu}$, although having the dimensions of a viscosity, is not a true state variable since it depends not only upon temperature but also on the geometry of the system. Still, Eqs. (3) can be interpreted as mathematically analogous to the equations of two-dimensional flow. Furthermore, Eqs. (3) can be solved by the method used in the viscous layer problem of Ref. 6 if \bar{v} can be taken as small compared to u^* . The present work

therefore extends the merged layer model of Ref. 6 only to slender bodies ($\theta_b \ll 1$) for which the viscous layer streamline curvature $\partial y^*/\partial x^*$ can be ignored and for which v^* is negligibly small compared to u^* . For such bodies, by Eq. (2a), $\bar{v} \ll u^*$.

With the governing equations in two-dimensional form and with $\bar{v} \ll u^*$, the analysis can more directly parallel that of Ref. 6. Following this reference, the viscous layer adjacent to the body is assumed locally similar, and for a calorically perfect gas with a Prandtl number of unity, Eqs. (3b) and (3c) then reduce to

$$(Nf_{nn})_n + ff_{nn} = 0 \quad (4a)$$

$$(N\textcircled{H})_n + f\textcircled{H}_n = 0 \quad (4b)$$

where

$$N = \rho_b \bar{\mu} / \rho_b \bar{\mu}_b \quad (5)$$

and where the dimensionless independent and dependent variables are

$$\eta = \frac{u_s^*}{(2\xi)^{1/2}} \int_0^{\bar{y}} \rho d\bar{y} \quad \xi(\bar{x}) = \int_0^{\bar{x}} \rho_b \bar{\mu}_b u_s^* d\bar{x} \quad (6)$$

$$f(\eta) = \int_0^{\eta} \frac{u^*}{u_s^*} d\eta \quad \textcircled{H}(\eta) = \frac{\bar{H} - \bar{H}_b}{\bar{H}_s - \bar{H}_b}$$

Here \bar{H} is the total enthalpy in the barred system (with $\bar{v} \ll u^*$) and

the subscripts "s" and "b" denote quantities at the shock surface and body surface, respectively.

Following Ref. 6, we first consider the problem neglecting velocity slip and temperature jump at the body surface. With the body temperature T_b constant, the boundary conditions are then

$$\begin{aligned} f = f_\eta = 0 \quad \textcircled{H} = 0 \quad \text{at } \eta = 0 \\ f_\eta = 1 \quad \textcircled{H} = 1 \quad \text{at } \eta = \eta_s \end{aligned} \tag{7}$$

Consider now the energy equation (4b) which is satisfied by the Crocco integral $\textcircled{H} = f_\eta$. From the definition of total enthalpy (with $\bar{v} \ll u^*$)

$$\frac{T}{T_b} = (1 - f_\eta) \left[1 + A^2 \left(\frac{T_0}{T_b} \right) f_\eta \right] \tag{8}$$

where

$$A(\bar{x}) = u_s^*/U_\infty \tag{9}$$

with U_∞ the freestream velocity. For the hypersonic conditions considered, the freestream stagnation temperature T_0 is given by

$$T_0 = U_\infty^2 / 2c_p.$$

Consider next the viscous layer momentum equation (4a). An expression for N is sought so that Eq. (4a) can be expressed in terms of the streamfunction $f(\eta)$ and its derivatives and in terms

of the local boundary conditions at the shock surface and the body. As shown in Pan and Probstein⁴, the normal pressure gradient across the viscous layer is negligible when viscous layer streamline curvature is negligible. Thus, by $p = \rho RT$, $\rho_b/\rho = T/T_b$ so that from the definition of η [Eq. (6)] it follows from Eq. (8) that at any given \bar{x}

$$\bar{y} = [(2\xi)^{1/2}/\rho_b u_s^*] I(\eta) \quad (10)$$

where

$$I(\eta) = \int_0^\eta (1 - f_\eta) [1 + A^2(T_0/T_b) f_\eta] d\eta \quad (11)$$

Hence, from Eq. (10) and from the definition of $\bar{\mu}$ [Eq. (2)]

$$\bar{\mu}/\mu = 1 + BI(\eta) \quad (12)$$

where B is a function of the boundary conditions at $\eta = 0$ and $\eta = \eta_s$. Since $N = (\rho/\rho_b)(\bar{\mu}/\bar{\mu}_b) = (T_b/T)(\bar{\mu}/\bar{\mu}_b) = (T_b/T)(\mu/\mu_b)(\bar{\mu}/\mu)$ and if a viscosity-temperature relation of the form $\mu \propto T^{1/2}$ is assumed, then by Eq. (12)

$$N = (T_b/T)^{1/2} [1 + BI(\eta)] \quad (13)$$

To complete this expression for N, we now obtain B in terms of the local boundary conditions at the shock surface and the body. This is done by first applying local conservation of mass flux

across the shock and into the viscous layer by use of

$$\rho_{\infty} U_{\infty} \sigma(j) = (2\pi L)^j \int_0^{\bar{y}_s} \rho u_s^* d\bar{y} = (2\pi L)^j (2\zeta)^{1/2} f(\eta_s) \quad (14a)$$

where $\sigma(j)$ is the cross-section of the incident streamtube given by

$$\sigma(j = 0) = [1 + \frac{1}{2} (\cot \theta_s - \tan \theta_b) \sin 2\theta_b] y_s^* / \cos \theta_b \quad (14b)$$

$$\sigma(j = 1) = \pi r_s^2 \quad (14c)$$

Now, from the definitions of \bar{x} [Eq. (2)] and of $\xi(\bar{x})$ [Eq. (6)], it can be shown that

$$2\xi = 2\rho_t \mu_b u_s^* [(1 - 2j/3) (r_b/L)^{2j}] x^* \quad (15)$$

where $r_b = x^* \sin \theta_b$ [see Fig. 2] has been used. Next, dividing Eq. (14a) by Eq. (15) for the case $j = 1$, Eq. (10) becomes

$$\bar{y} = \{ [2\mu_b f(\eta_s) / \rho_{\infty} U_{\infty}] (\pi_b / r_s)^2 (2x^* / 3L) \} I(\eta) \quad (16)$$

Finally, neglecting longitudinal shock curvature, we set

$y_s^* / x^* = \tan \theta_s$ so that

$$r_s / x^* = (r_b + y_s^* \cos \theta_b) / x^* = [1 + (\tan \theta_s / \tan \theta_b)] \sin \theta_b \quad (17)$$

and by comparing Eq. (12) to the definition (2b) of $\bar{\mu}$ by the use of Eqs. (16) and (17), we find

$$B = \{8j\mu_b/3\mu_\infty \tan \theta_b [1 + (\tan \theta_s/\tan \theta_b)]^2\} f(\eta_s) \alpha \quad (18)$$

Here α is the inverse Reynolds number $(\rho_\infty U_\infty r_b/\mu_\infty)^{-1}$ based on free-stream conditions and the local radius $r_b(x^*)$ of transverse body curvature. From Eq. (18), B vanishes for two-dimensional flow ($j = 0$).

From the energy equation in the form of Eq. (8), from $\mu \sim T^{1/2}$, and from Eqs. (13) and (16) which together relate the parameter N to the streamfunction $f(\eta)$, to its derivatives, and to the local boundary conditions on the viscous layer, the viscous layer momentum equation (4a) now reduces to

$$\left[\frac{\{1 + C_2 I(\eta)\} f_{\eta\eta}}{\{(1 - f_\eta)[1 + C_1 f_\eta]\}^{1/2}} \right]_\eta + ff_{\eta\eta} = 0 \quad (19)$$

where

$$C_1 = A^2(T_0/T_b) \quad (20a)$$

$$C_2 = \{8j(\frac{\gamma-1}{2} \frac{T_b}{T_0})^{1/2} f(\eta_s)/3 \tan \theta_b [1 + (\tan \theta_s/\tan \theta_b)]^2\} M_\infty \alpha \quad (20b)$$

Equation (19) differs from the reduced viscous layer momentum equation of Ref. 6 only by the appearance of the new term $C_2 I(\eta)$. This term

introduces the effects of transverse curvature characterized by the parameter $M_\infty \alpha$, and it vanishes for the case of two-dimensional flow. For the case of axial symmetric flow, only the regime $M_\infty \alpha \ll 1$ is treated in this work. The reason for this will be discussed in conjunction with the shock structure analysis.

Now, if C_1 and C_2 were to be treated as parameters, then for each value of $(f_{\eta\eta})_b$ greater than the value which gives the boundary layer solution ($\eta_s \rightarrow \infty$), a viscous layer solution would be obtained with finite shear (proportional to $Nf_{\eta\eta}$) at the shock surface $\eta = \eta_s$ where $f_\eta = u^*/u_s^* = 1$. The shock surface coordinates x^* , y_s^* corresponding to η_s are determined by 1) employing Eq. (14a) which states that mass flux into the viscous layer between the body and shock surface is conserved and 2) by matching the velocity u^* and its gradient $\partial u^*/\partial y^*$ obtained with finite shear at the outer edge of the viscous layer to the respective quantities obtained at the inner edge of the shock from the shock structure solution.

III. Shock Structure

Since the flow at the shock surface has been assumed locally similar within the viscous layer model, all shock structure variables at the inner edge of the shock are single-valued functions of η_s .

The shock transition equations in the coordinate frame centered at the shock surface are illustrated by the continuity and tangential momentum equations

$$\frac{\partial}{\partial n} (r^j \rho v) = 0 \quad (21a)$$

$$\rho v \frac{\partial u}{\partial n} = \frac{1}{r^j} \frac{\partial}{\partial n} (r^j \mu \frac{\partial u}{\partial n}) \quad (21b)$$

where n is the coordinate in the direction measured normal from the shock surface to the freestream, and the velocity components u and v are taken normal to and parallel to n , respectively [see Fig. 2]. Based on the results of Ref. 6, the effects of including longitudinal shock curvature terms in Eqs. (21) have been neglected as small.

Integrating the continuity equation (21a) yields

$$r^j \rho v = \text{constant} = r_s^j \rho_s v_s = r_\infty^j \rho_\infty v_\infty \quad (22a)$$

Substituting Eq. (22a) into Eq. (21b) and multiplying by $(r/r_s)^{2j}$, the tangential momentum equation (21b) becomes

$$\rho_s v_s \left(\frac{r}{r_s}\right)^j \frac{\partial u}{\partial n} = \left(\frac{r}{r_s}\right)^j \frac{\partial}{\partial n} \left[\mu \left(\frac{r}{r_s}\right)^j \frac{\partial u}{\partial n} \right] \quad (22b)$$

To solve these shock structure equations, the following reduced, dimensionless variables are introduced:

$$\begin{aligned} \zeta &= \int_0 \frac{\rho_\infty U_\infty}{\mu} \left(\frac{r_s}{r}\right)^j dn & W &= \frac{u}{U_\infty} & V &= \frac{v}{U_\infty} \\ P &= \frac{p}{\rho_\infty U_\infty^2} & D &= \frac{\rho}{\rho_\infty} & \phi &= \frac{h + \frac{1}{2} v^2}{U_\infty^2} \end{aligned} \quad (23)$$

The dimensionless forms of Eqs. (22) by (23) are then

$$D_s V_s = [1 + j(\Delta_s/r_s)] D_\infty V_\infty \quad (24a)$$

$$\frac{\partial^2 W}{\partial \zeta^2} - D_s V_s \frac{\partial W}{\partial \zeta} = 0 \quad (24b)$$

where $\Delta_s \equiv (r_\infty - r_s)$ denotes shock thickness. Equations (24) differ from the "zero-order" shock transition equations of Ref. 6 only by the appearance of the transverse shock curvature parameter Δ_s/r_s . If however $M_\infty \ll 1$, then $\Delta_s/r_s \ll 1$ and a simple closed form solution to Eqs. (24) can be readily obtained analogous to the "zero-order" shock solution in Ref. 6. In the present model, $M_\infty \ll 1$ is satisfied and transverse shock curvature terms are neglected as small in the shock structure equations. Equations (24) then become

$$D_s V_s = D_\infty V_\infty \quad (25a)$$

$$\frac{\partial^2 W}{\partial \zeta^2} - D_s V_s \frac{\partial W}{\partial \zeta} = 0 \quad (25b)$$

and in similar manner the normal momentum equation and the energy equation for the shock structure become

$$D_s V_s \frac{\partial V}{\partial \zeta} + \frac{\partial P}{\partial \zeta} - \frac{4}{3} \frac{\partial^2 V}{\partial \zeta^2} = 0 \quad (25c)$$

$$D_s V_s \frac{\partial \phi}{\partial \zeta} - \frac{4}{3} \frac{\partial^2 \phi}{\partial \zeta^2} + D_s V_s W \frac{\partial W}{\partial \zeta} - \frac{\partial W}{\partial \zeta} (W \frac{\partial W}{\partial \zeta}) = 0 \quad (25d)$$

The shock structure is taken to extend from the outer edge of the viscous layer $\zeta = 0$ to the freestream $\zeta \rightarrow \infty$. At the shock surface, the shock structure flow variables and their normal gradients are required to match the corresponding viscous layer values at $\eta = \eta_s$ as given by the solution to Eq. (19).

Following Ref. 6, we now illustrate this matching procedure at the shock surface for the case of the finite tangential shear stress $\mu_s \left(\frac{\partial u^*}{\partial y^*} \right)_s$. In terms of viscous layer variables, this stress may be written

$$\mu_s \left(\frac{\partial u^*}{\partial y^*} \right)_s = (\mu/\bar{\mu})_s \cdot \left(\frac{\partial \bar{y}}{\partial y^*} \right)_s \cdot \left(\bar{\mu} \frac{\partial u^*}{\partial \bar{y}} \right)_s \quad (26)$$

or

$$\left(\mu \frac{\partial u^*}{\partial y^*} \right)_s = Q_1(j) Q_2(j) \rho_\infty U_\infty^2 \left(\frac{Nf}{2f} \right)_s \quad (27)$$

where

$$Q_1(j) = \begin{cases} \left[1 + \frac{1}{2} (\cot \theta_s - \tan \theta_b) \sin 2\theta_b \right] (\tan \theta_s / \cos \theta_b) & \text{for } j = 0 \\ \left[1 + (\tan \theta_s / \tan \theta_b) \right]^2 (3L/2x^*) & \text{for } j = 1 \end{cases} \quad (28)$$

$$Q_2(j) = \left(\frac{\sin \theta_b (1 + \tan \theta_s / \tan \theta_b) (x^*/L)}{1 + 2(\tan \theta_s / \tan \theta_b) [1 + (\tan \theta_s / 2 \tan \theta_b)]} \right)^j \quad (29)$$

On the other hand, at the inner edge of the shock, the shear is

$$\left(u \frac{\partial u^*}{\partial y^*}\right)_s = \rho_\infty U_\infty^2 \left(\frac{\partial W}{\partial \zeta}\right)_s \left(\frac{\partial n}{\partial y^*}\right)_s \left(\frac{\partial u^*}{\partial u}\right)_s = \rho_\infty U_\infty^2 \left(\frac{\partial W}{\partial \zeta}\right)_s \quad (30)$$

with the subscript "s" here denoting conditions at $\zeta = 0$. Equating Eq. (27) to Eq. (30)

$$\left(\frac{\partial W}{\partial \zeta}\right)_s = Q_1(j) Q_2(j) A \left(\frac{Nf}{2f}\right)_s \quad (31)$$

This matching of viscous layer solution to shock structure solution at the shock surface is shown next for the case of the shock surface velocity u_s^* . First, recognizing from Fig. 2 that at the freestream $W_\infty = \cos(\theta_s + \theta_b)$ and $V_\infty = -\sin(\theta_s + \theta_b)$, and at the shock surface $W_s = (u_s^*/U_\infty) (u_s/u_s^*) = A \cos \theta_s$, the tangential momentum equation (25b) is integrated once with the result

$$\left(\frac{\partial W}{\partial \zeta}\right)_s = [\cos(\theta_s + \theta_b) - A \cos \theta_s] \sin(\theta_s + \theta_b) \quad (32)$$

Substituting Eq. (32) into Eq. (31) and solving for the reduced velocity A at the shock surface

$$A = \frac{u_s^*}{U_\infty} = \left\{ \frac{\cos \theta_s}{\cos(\theta_s + \theta_b)} + \frac{2Q_1(j) Q_2(j)}{\sin[2(\theta_s + \theta_b)]} \left(\frac{Nf}{2f}\right)_s \right\}^{-1} \quad (33)$$

For the case of flat plate flow $j = 0$ and $\theta_b = 0$, Eq. (33) reduces to the result of Ref. 6.

The shock angle in terms of the density and pressure behind the shock is obtained next by integrating the normal momentum

equation (25c) once and applying freestream boundary conditions. Neglecting the gradient term $(\frac{\partial V}{\partial \zeta})_s$ as small compared to V_s [see Ref. 5]

$$\sin(\theta_s + \theta_b) V_s = P_s - \sin^2(\theta_s + \theta_b) - \frac{1}{\gamma M_\infty^2} \quad (34)$$

Eliminating V_s by means of Eq. (25a), the shock angle is then given by

$$\sin^2(\theta_s + \theta_b) = D_s (P_s - 1/\gamma M_\infty^2) / (D_s - 1) \quad (35)$$

The reduced enthalpy behind the shock is sought next. Integrating Eq. (25b) twice, substituting the resulting velocity profile $W(\zeta)$ into the energy equation (25d), and integrating twice, we obtain the result

$$\begin{aligned} \phi_s = \frac{1}{2} \{ [1 - A \cos \theta_s / \cos(\theta_s + \theta_b)]^2 \cos^2(\theta_s + \theta_b) \\ + \sin^2(\theta_s + \theta_b) + 2/(\gamma - 1) M_\infty^2 \} \end{aligned} \quad (36)$$

where the gradient term $(\frac{\partial \phi}{\partial \zeta})_s$ has been neglected compared to ϕ_s [see Ref. 5], and where the term $(\frac{\partial W}{\partial \zeta})_s$ has been eliminated by use of Eq. (32).

In order to obtain the density ratio across the shock, another expression for $\sin^2(\theta_s + \theta_b)$ is first found by substituting ϕ_s

from Eq. (36) and V_s from Eq. (25a) into the reduced equation of state

$$P_s = \frac{\gamma - 1}{2\gamma} D_s (2\phi_s - V_s^2) \quad (37)$$

Equating the resulting expression to Eq. (35)

$$D_s = \frac{\rho_s}{\rho_\infty} = \frac{[(\gamma + 1)/(\gamma - 1)] P_s + 1/\gamma M_\infty^2}{P_s + [1 - A \cos \theta_s / \cos (\theta_s + \theta_b)]^2 + (1/\gamma M_\infty^2)(\gamma + 1)/(\gamma - 1)} \quad (38)$$

We note here that in order to avoid the solution of a cubic equation, a term $D_s^2 [1 - A \cos \theta_s / \cos (\theta_s + \theta_b)]^2$, which appears after equating the expressions for $\sin^2 (\theta_s + \theta_b)$, has been neglected in comparison with $(D_s^2 - 1)$. This is justified on the basis that since the reduced shear $(Nf_{\eta\eta})_s$ is finite but always small compared to unity, then by Eq. (33) $A \cos \theta_s = W_s$ is always close to $W_\infty = \cos (\theta_s + \theta_b)$; and the larger D_s , the closer W_s is to W_∞ . This is borne out by the numerical results.

The reduced pressure $P_s[\eta_s(\bar{x})]$ at the shock surface has, as stated before in conjunction with Eq. (10), been assumed equal to the reduced pressure $P_b(\bar{x})$ on the body at the same value of \bar{x} . From Eq. (10) written in the form

$$\bar{y}_s = \{(2\xi)^{1/2} T_b / (\rho_s u_s^* T_s)\} I(\eta_s) \quad (39)$$

and from the definition of \bar{y} [Eq. (2a)] written in the form

$$\bar{y}_s = \int_0^{y_s^*} [(r_b + y_s^* \cos \theta_b)/L]^j dy^* = [(r_s + r_b) x^* \tan \theta_s / 2Ly_s^*]^{\frac{1}{j}} y_s^* \quad (40)$$

we have upon elimination of \bar{y}_s and the use of Eq. (14)

$$P_s = P_b = \frac{P_b}{\rho_\infty U_\infty^2} = Q_1(j) Q_3(j) \frac{\gamma - 1}{2\gamma} \left(\frac{F}{A}\right) \quad (41)$$

where

$$Q_3(j) = \begin{cases} \cot \theta_s & \text{for } j = 0 \\ \frac{2(x^*/L) \cos \theta_b}{3[2 + (\tan \theta_s / \tan \theta_b)] (\tan \theta_s / \tan \theta_b)} & \text{for } j = 1 \end{cases} \quad (42)$$

and where

$$F = \frac{T_b}{T_0} \frac{I(\eta_s)}{f(\eta_s)} \quad (43)$$

Therefore, if from Eq. (19) a streamfunction $f(\eta)$ and its derivatives were to be known at $\eta = \eta_s$, the relations (33), (35), (38) and (41) would form a closed system of four equations in the four unknowns A , θ_s , D_s , and P_s .

IV. Method of Calculation

The model as formulated imposes the following restrictions on the input gas and body properties: M_∞ sufficiently large such that $c_p T_0 \gg U_\infty^2/2$, $T_b/T_0 \ll 1$, $\gamma = \text{constant}$, $Pr = 1$, and $\theta_b \ll 1$.

The solution for the viscous layer streamfunction $f(\eta)$ and for the various flow properties of interest proceeds by first

transforming Eq. (19) to the following set of first order differential equations as in Ref. 6:

$$f_{\eta} = J \quad J_{\eta} = z^{1/2}(1 + c_2 I)^{-1} g \quad g_{\eta} = -z^{1/2}(1 + c_2 I)^{-1} f g \quad (44)$$

where

$$z = |1 - J| (1 + c_2 J) \equiv I_{\eta} \quad (45)$$

The no-slip boundary conditions

$$f(0) = J(0) = I(0) = 0 \quad \text{at } \eta = 0 \quad (46)$$

$$J(\eta_s) = 1 \quad \text{at } \eta = \eta_s$$

are then imposed. Now, for values of the wall shear $g(0) = (f_{\eta\eta})_b$ greater than the value which gives an inviscid flow region at the outer edge of a boundary layer ($\eta_s \rightarrow \infty$), a velocity profile with finite shear $g(\eta_s) = (Nf_{\eta\eta})_s$ at the shock surface can be obtained for each station along the body within the merged layer. At each such value of $g(0)$, the no-slip boundary conditions are fully specified. Beginning then at $\eta = 0$ with a value $g(0) = [g(0)]_{\eta_s \rightarrow \infty}^+$ only slightly larger than the value $[g(0)]_{\eta_s \rightarrow \infty}$ which gives the boundary layer solution ($\eta_s \rightarrow \infty$), Eqs. (44) - (45) are simultaneously integrated out from the body surface to the shock surface for fixed

local values of C_1 and C_2 . The initial guesses for these parameters are obtained from the boundary layer limit $\eta_s \rightarrow \infty$ with θ_s guessed to be $\theta_s = \theta_{s_{inv}}$ where $\theta_{s_{inv}} = \theta_{s_{inv}}(\gamma, M_\infty, \theta_b, j)$ is the inviscid shock layer value for wedges and cones given in Ref. 12. As shown in the Appendix

$$C_1 \Big|_{\eta_s \rightarrow \infty} = \frac{r_0}{T_b} \left[\frac{\cos(\theta_{s_{inv}} + \theta_b)}{\cos \theta_{s_{inv}}} \right]^2 \quad (47)$$

$$\theta_s = \theta_{s_{inv}}$$

$$C_2 \Big|_{\eta_s \rightarrow \infty} = 0 \quad (48)$$

$$\theta_s = \theta_{s_{inv}}$$

The numerical integration of Eqs. (44) - (45) is stopped at the first point η reached within the viscous layer where $J = f_\eta = u^*/u_s^* \geq 1$. The coordinate η_s is the finite value of η at this point, and the resulting finite values of $f(\eta_s)$, $g(\eta_s)$ and $I(\eta_s)$ are used to compute A and F in approximate form from [see Eq. (33)]

$$A = \left[\frac{\cos \theta_{s_{inv}}}{\cos(\theta_{s_{inv}} + \theta_b)} + \frac{2Q_1(j) Q_2(j)}{\sin 2(\theta_{s_{inv}} + \theta_b)} \left(\frac{g}{2f} \right)_{\eta=\eta_s} \right]^{-1} \quad (49)$$

and the relation given by Eq. (43). These results are then used to provide a better value of θ_s from Eqs. (35), (38) and (41). Better values for the local parameters C_1 and C_2 are next obtained from

the relations [see Appendix]

$$C_1 = \frac{T_0}{T_b} \left\{ \frac{\cos \theta_s}{\cos (\theta_s + \theta_b)} + \frac{2Q_1(j) Q_2(j)}{\sin [2(\theta_s + \theta_b)]} \left(\frac{g}{2f} \right)_{\eta=\eta_s} \right\}^{-2} \quad (50)$$

$$C_2 = \frac{[2 + (\tan \theta_s / \tan \theta_b)] (\tan \theta_s / \tan \theta_b)}{I(\eta_s) f(\eta_s)} \quad (51)$$

and beginning again at $\eta = 0$ with $g(0) = [g(0)]_{\eta_s}^+ \rightarrow \infty$, Eqs. (44) - (45) are re-integrated from the body to the shock surface $\eta = \eta_s$. When after such successive iterations the results at the shock surface from one cycle agree sufficiently with those values from the previous cycle, the local no-slip viscous layer solution is available. The effects of small local velocity slip and temperature jump are then computed as local perturbations from the no-slip results. The method for obtaining the local slip solution is entirely analogous to that given in Ref. 6 except that Eqs. (47) - (48) of that reference are replaced by

$$\frac{u_{sl}^*}{u_s^*} = (f_{\eta})_b \left[\frac{\sin \theta_b}{(3L/x^*)} \right]^j \left[\left(1 - \frac{2j}{3} \right) Q_{3_{nsl}}(j) \right]^{-1} \left[\frac{\pi \gamma}{(\gamma - 1)} \frac{T_b}{T_0} \right]^{1/2} \cdot \left[\frac{A_{nsl}}{2f_{nsl} F_{nsl}} \right]_{\eta=\eta_s} [(f_{nsl})_{\eta\eta}]_{\eta=0} \quad (52)$$

$$A_{sl} \approx \left\{ \frac{\cos \theta_{s_{nsl}}}{\cos (\theta_{s_{nsl}} + \theta_b)} + \frac{f_{nsl}}{f} \left[\frac{1}{A_{nsl}} - \frac{\cos \theta_{s_{nsl}}}{\cos (\theta_{s_{nsl}} + \theta_b)} \right] \right\}_{\eta=\eta_s}^{-1} \quad (53)$$

and the rarefaction parameter [Eq. (35) of Ref. 6] is replaced by

$$\frac{M_\infty C^{1/2}}{Re_{x^*,\infty}^{1/2}} = \left[\frac{Q_1(j)}{(1 - \frac{2j}{3}) Q_3(j)(\gamma - 1) F} \right]^{1/2} \left[\frac{x^* \sin \theta_b}{3L} \right]^j / f(\eta_s) \quad (54)$$

The final results at $g(0) = [g(0)]_{\eta_s \rightarrow \infty}^+$ constitute the local solution at the downstream end of the merged layer. The final values there for C_1 and C_2 become the initial guesses for these parameters at the adjacent station a small distance upstream. The viscous layer equations are integrated here from $\eta = 0$ with $g(0) = [g(0)]_{\eta_s \rightarrow \infty}^+ + \Delta g(0)$, where $\Delta g(0)$ is a small increment in the surface shear $g(0)$. Through this stepwise upstream marching method, with successive iteration cycles at each step, the velocity and state variables are computed at several stations x^* within the merged layer regime. The computation is stopped at the upstream end when the condition $M_\infty \alpha \ll 1$ or the condition $(f_\eta)_b \ll 1$ is no longer satisfied. If the computation is carried to stations x^* farther upstream, the present model breaks down as the calculated values of ρ_s/ρ_∞ become less than unity. This occurs at values of the rarefaction parameter $M_\infty (C/Re_{x^*,\infty})^{1/2}$ of the order of unity.

VI. Results and Discussion

Computations have been carried out in the manner indicated in the previous section. The cases considered cover the range $20 \leq M_\infty \leq 25$, $0.06 \leq T_b/T_0 \leq 0.15$ and $0^\circ \leq \theta_b \leq 20^\circ$.

In Figs. 3 - 5 the density at the shock surface for sharp wedges is compared with measured values obtained by McCroskey, Bogdonoff and Genchi¹⁴. Considering the scatter in the data, the agreement with theory would appear to be good. The theoretical shock density ratio for a 10° cone is shown compared with the data in Fig. 6. In contrast with a wedge having the same flow conditions and comparable angle θ_b , the shock at the same distance x^* from the leading edge is weaker on the cone. This is due to the circumferential spreading of the flow around the cone, bringing the shock wave closer to the body surface and causing the merged layer to extend farther downstream than on the wedge.

Fig. 7 presents the wedge surface pressures given by Vidal and Bartz⁹ in comparison with the theory for several values of θ_b . The strong interaction and free molecule limits given by Hayes and Probstein¹³ are also shown. Both the present theory and the data lie below the result predicted by strong interaction theory. This is also seen to be true for sharp cones as shown in Fig. 8 where the cone surface pressure by the present theory and by the strong interaction theory of Mirels and Ellinwood¹⁹ are compared to the experimental data in the form presented by Waldron¹⁷ and by Hofland and Glick¹⁸.

On Figs. 9 - 10 the experimental skin friction and heat transfer data obtained by Vidal and Bartz⁹ on wedges is compared with the theory, and the agreement appears to be quite good. The theoretical result for cones is given in Fig. 11 compared to experiment in the form presented by Waldron¹⁷.

In view of the reasonable agreement of experimental data with the theory it would appear that the present continuum merged layer model is a satisfactory one up to rarefaction parameters $M_\infty (C/Re_{x^*,\infty})^{1/2} \sim 1$. This limit would correspond to distances back from the leading edge of the order of M_∞ mean free paths.

Appendix

THE PARAMETERS C_1 AND C_2

By Eq. (33), the parameter C_1 is

$$C_1 = A^2 \frac{T_0}{T_b} = \frac{T_0}{T_b} \left[\frac{\cos \theta_s}{\cos(\theta_s + \theta_b)} + \frac{2Q_1(j) Q_2(j)}{\sin[2(\theta_s + \theta_b)]} \left(\frac{g}{2f} \right)_{\eta=\eta_s} \right]^{-2} \quad (A-1)$$

To find C_2 , an expression for the parameter $M_\infty \alpha$ is first required. To obtain this, we eliminate ξ between Eqs. (14) and (15) for the case of $j = 1$ and note that $\rho_b \mu_b / \rho_\infty \mu_\infty = \gamma M_\infty P_s 2T_0 / (\gamma - 1) T_b^{1/2}$ from $\mu \propto T^{1/2}$ and the equation of state, with the result

$$M_\infty \alpha = \frac{3 \cos \theta_b (\tan \theta_s + \tan \theta_t) [1 + (\tan \theta_s / \tan \theta_b)]^2}{8 \gamma P_s A f^2(\eta_s)} \left[\frac{\gamma - 1}{2} \frac{T_b}{T_0} \right]^{1/2} \quad (A-2)$$

Using Eqs. (28) and (41) - (43) to eliminate P_s , we obtain then

$$C_2 = [2 + (\tan \theta_s / \tan \theta_b)] (\tan \theta_s / \tan \theta_b) / I(\eta_s) f(\eta_s) \quad (A-3)$$

from Eq. (20b).

In the boundary layer limit $\eta_s \rightarrow \infty$ and $g(\eta_s) \rightarrow 0$, we find that since $f_\eta \sim 1$ when $\eta \sim \eta_s$

$$[f(\eta_s)]_{\eta_s \rightarrow \infty} = \left[\int_0^{\eta_s} f_\eta d\eta \right]_{\eta_s \rightarrow \infty} \rightarrow \infty \quad (A-4)$$

$$[I(\eta_s)]_{\eta_s \rightarrow \infty} = \left[\int_0^{\eta_s} (1 - f_\eta) (1 + C_1 f_\eta) d\eta \right]_{\eta_s \rightarrow \infty} = \text{finite} \quad (A-5)$$

so that taking $\theta_s = \theta_{s_{inv}}$, Eqs. (A-1) and (A-3) yield

$$C_1 \Big|_{\eta_s \rightarrow \infty} = \frac{T_0}{T_b} \left[\frac{\cos(\theta_{s_{inv}} + \theta_b)}{\cos \theta_{s_{inv}}} \right]^2 \quad (A-6)$$

$\theta_s = \theta_{s_{inv}}$

$$C_2 \Big|_{\eta_s \rightarrow \infty} = 0 \quad (A-7)$$

$\theta_s = \theta_{s_{inv}}$

Here $\theta_{s_{inv}}(\gamma, M_\infty, \theta_b, j)$ is the inviscid shock layer value for θ_s obtained from Ref. 12.

References

1. Rudman, S. and Rubin, S. G., "Hypersonic Flow Over Slender Bodies With Sharp Leading Edges," AIAA J., Vol. 6, No. 10, Oct. 1968, pp. 1883-1890.
2. Rubin, S. C., Lin, T. C., Pierucci, M. and Rudman, S., "Hypersonic Interactions Near Sharp Leading Edges," AIAA J., Vol. 7, No. 9, Sept. 1969, pp. 1744-1751.
3. Cheng, H. K., Chen, S. Y., Mobly, R. and Huber, C., "On the Hypersonic Leading-Edge Problem in the Merged Layer Regime," Rarefied Gas Dynamics, Supplement 5, Vol. I, edited by L. Trilling and H. Wachman, Academic Press, N. Y., 1969, pp. 451-463.
4. Pan, Y. S. and Probstein, R. F., "Rarefied Flow Transition at a Leading Edge," Fundamental Phenomena in Hypersonic Flow, Cornell University Press, Ithaca, N. Y., 1966, pp. 259-306.
5. Oguchi, H., "Shock Wave and Viscous Layer Structure in a Rarefied Hypersonic Flow Near the Leading Edge of a Sharp Flat Plate," Report 418, Institute of Space and Aero. Sciences, Univ. of Tokyo, Tokyo, Japan, 1967.
6. Shorenstein, M. L. and Probstein, R. F., "The Hypersonic Leading Edge Problem," AIAA J., Vol. 6, No. 10, Oct. 1968, pp. 1898-1906.
7. McCroskey, W. J., Bogdonoff, S. M. and McDougall, J. G., "An Experimental Model for the Sharp Flat Plate in Rarefied Hypersonic Flow," AIAA J., Vol. 4, No. 9, Sept. 1966, pp. 1580-1587.
8. Harbour, P. J. and Lewis, J. H., "Preliminary Measurements of the Hypersonic Rarefied Flow Field on a Sharp Flat Plate Using an

Electron Beam Probe," Rarefied Gas Dynamics, Supplement 4, Vol. II, edited by C. L. Brundin, Academic Press, N. Y., 1967, pp. 1031-1046.

9. Vidal, R. J. and Bartz, J. A., "Surface Measurements on Sharp Flat Plates and Wedges in Low Density Hypersonic Flow," CAL No. AF-2041-A-2, Cornell Aero. Lab., Buffalo, N. Y., 1968.

10. Probststein, R. F. and Elliott, D., "The Transverse Curvature Effect in Compressible Axially Symmetric Laminar Boundary Layer Flow," J. of Aero. Sci., Vol. 23, No. 3, March 1956, p. 208.

11. Oguchi, H., "Leading Edge Slip Effects in Rarefied Hypersonic Flow," Rarefied Gas Dynamics, Supplement 2, Vol. II, edited by J. A. Laurmann, Academic Press, N. Y., 1963, pp. 181-193.

12. NACA Technical Report 1135, National Advisory Committee for Aeronautics, 1953.

13. Hayes, W. D. and Probststein, R. F., Hypersonic Flow Theory, Academic Press, N. Y., 1959.

14. McCroskey, W. J., Bogdonoff, S. M. and Genchi, A. P., "Leading Edge Flow Studies of Sharp Bodies in Rarefied Hypersonic Flow," Rarefied Gas Dynamics, Supplement 4, Vol. II, edited by C. L. Brundin, Academic Press, N. Y., 1967, pp. 1047-1066.

15. Vas, I. E., Iacavazzi, C., Carlomagno, G. and Bogdonoff, S. M., "Effect of Body Inclination on the Merging of a Hypersonic Low Density Flow Over Sharp Two-Dimensional Linear Bodies," Rarefied Gas Dynamics, Supplement 5, Vol. I, edited by L. Trilling and H. Wachman,

Academic Press, N. Y., 1969, pp. 501-508.

16. Feik, R. A., Genchi, A. and Vas, I. E., "A Study of Merging on Cones," Rarefied Gas Dynamics, Supplement 5, Vol. I, edited by L. Trilling and H. Wachman, Academic Press, N. Y., 1969, pp. 493-499.

17. Waldron, H. F., "Viscous Hypersonic Flow Over Pointed Cones at Low Reynolds Numbers," AIAA J., Vol. 5, No. 2, Feb. 1967, pp. 208-218.

18. Hofland, R. and Glick, H. S., "Low Density Hypersonic Flow Over a Cone," AIAA J., Vol. 8, No. 1, Jan. 1970, pp. 52-59.

19. Mirels, H. and Ellinwood, J. W., "Hypersonic Viscous Interaction Theory for Slender Axisymmetric Bodies," AIAA J., Vol. 6, No. 11, Nov. 1968, pp. 2061-2070.

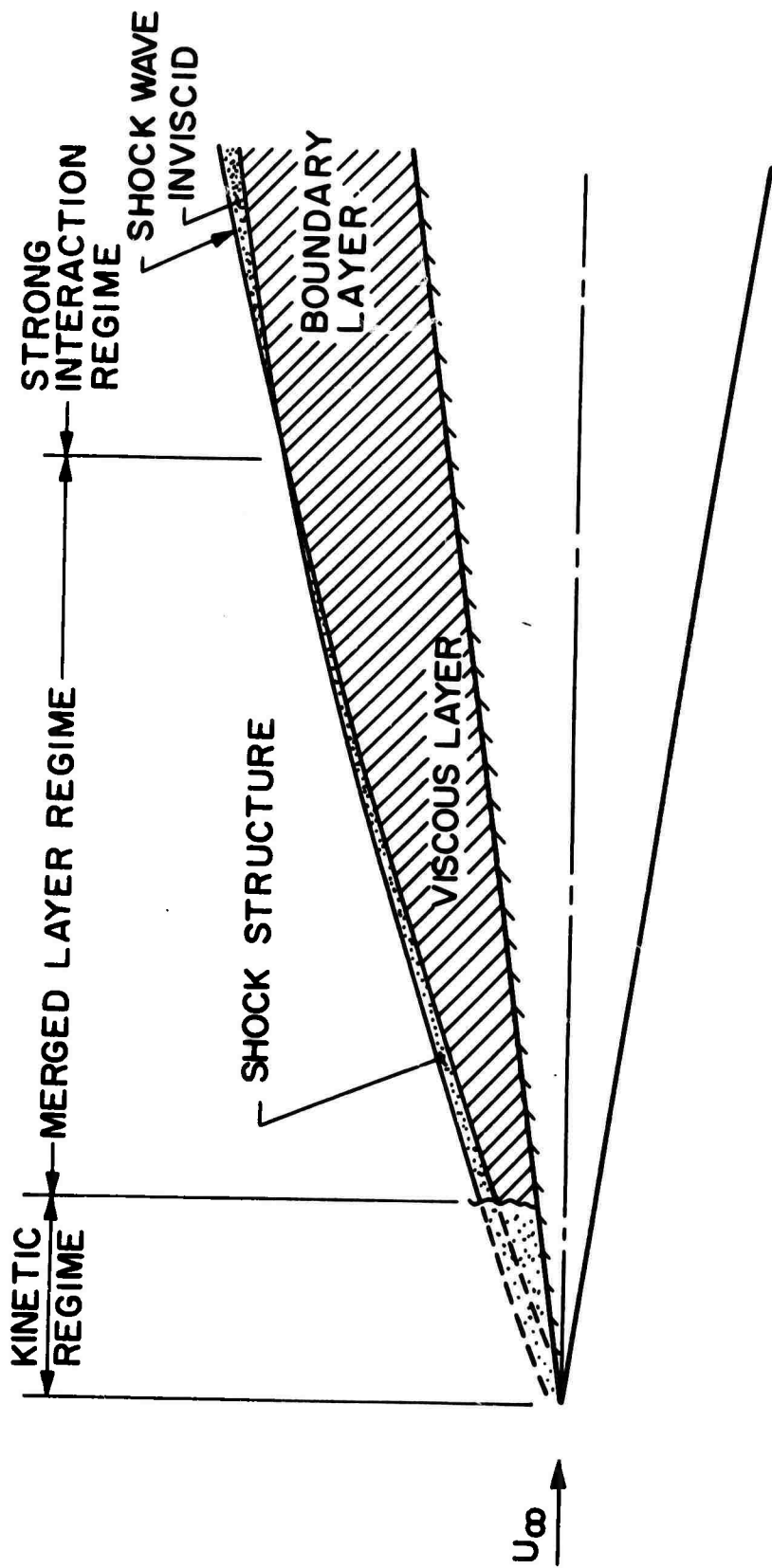


Fig. 1 Leading edge flowfield

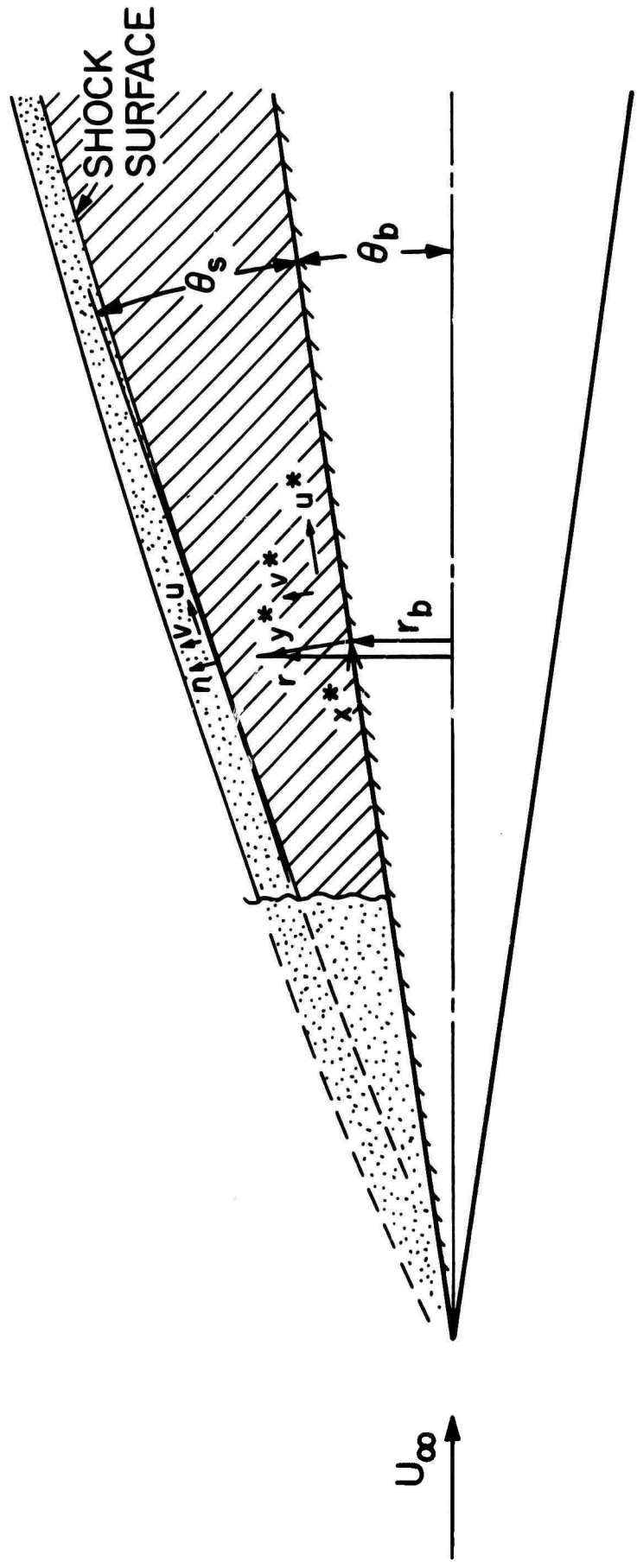


Fig. 2 Merged layer detail

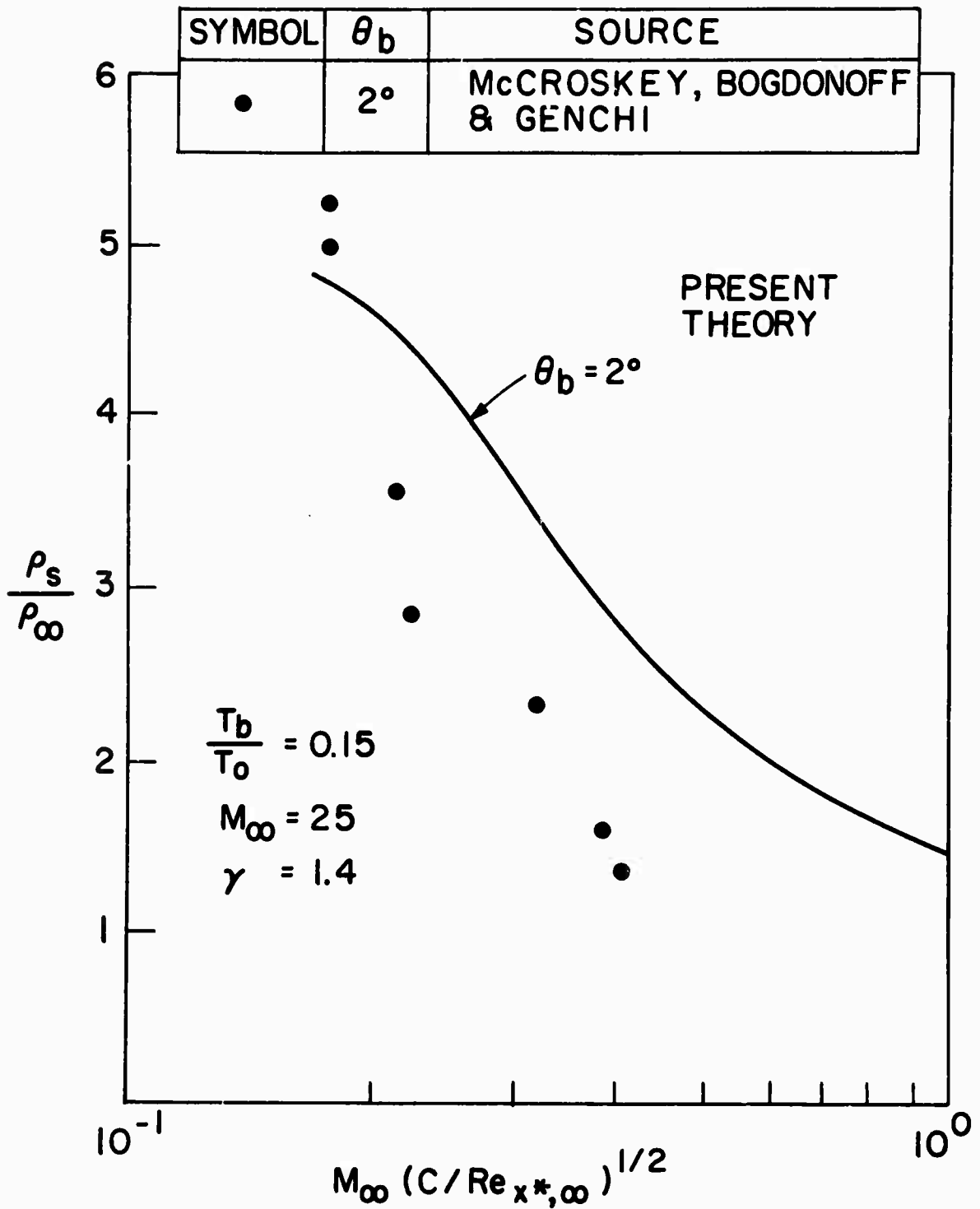


Fig. 3 Density ratio across the shock structure for a wedge

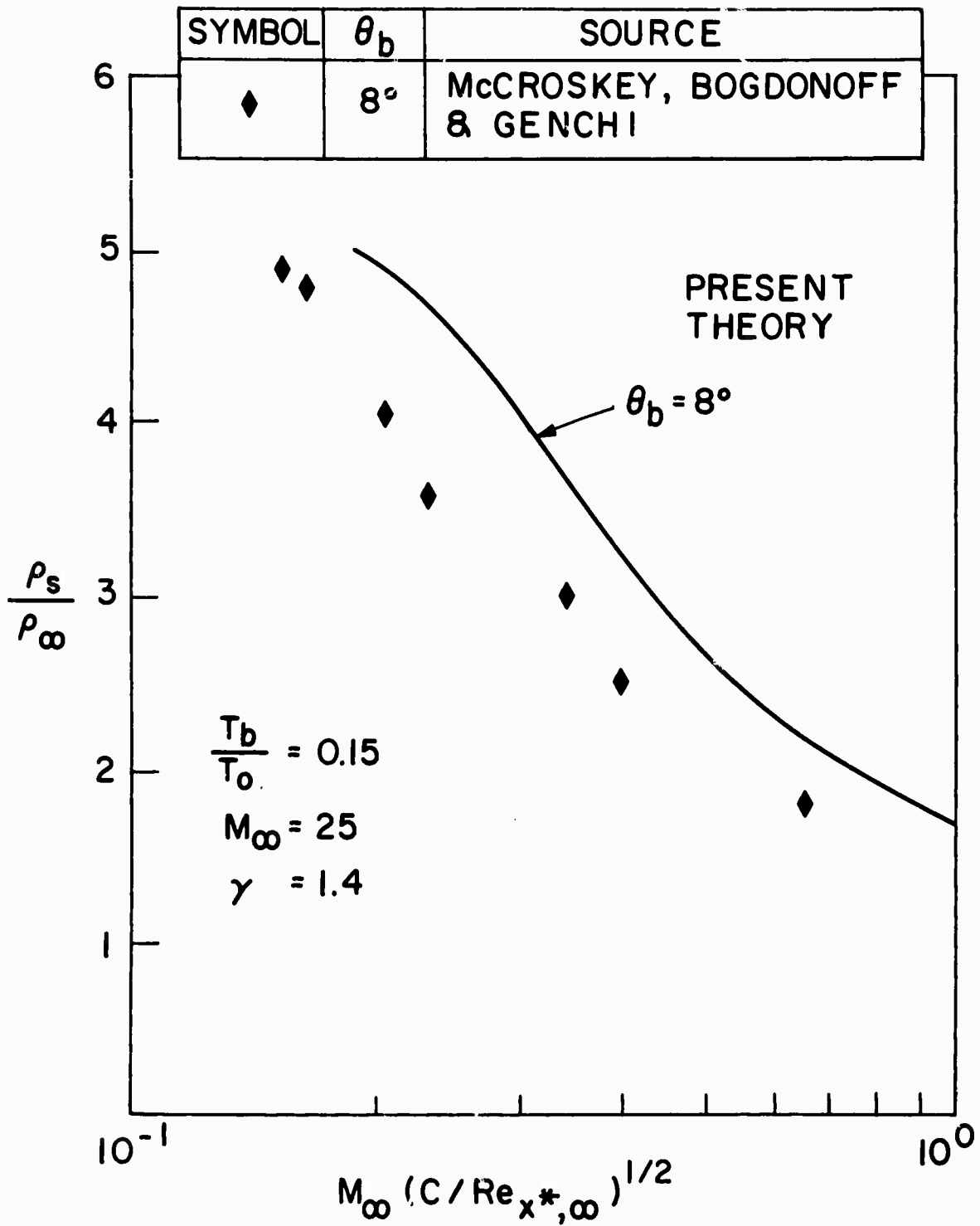


Fig. 4 Density ratio across the shock structure for a wedge

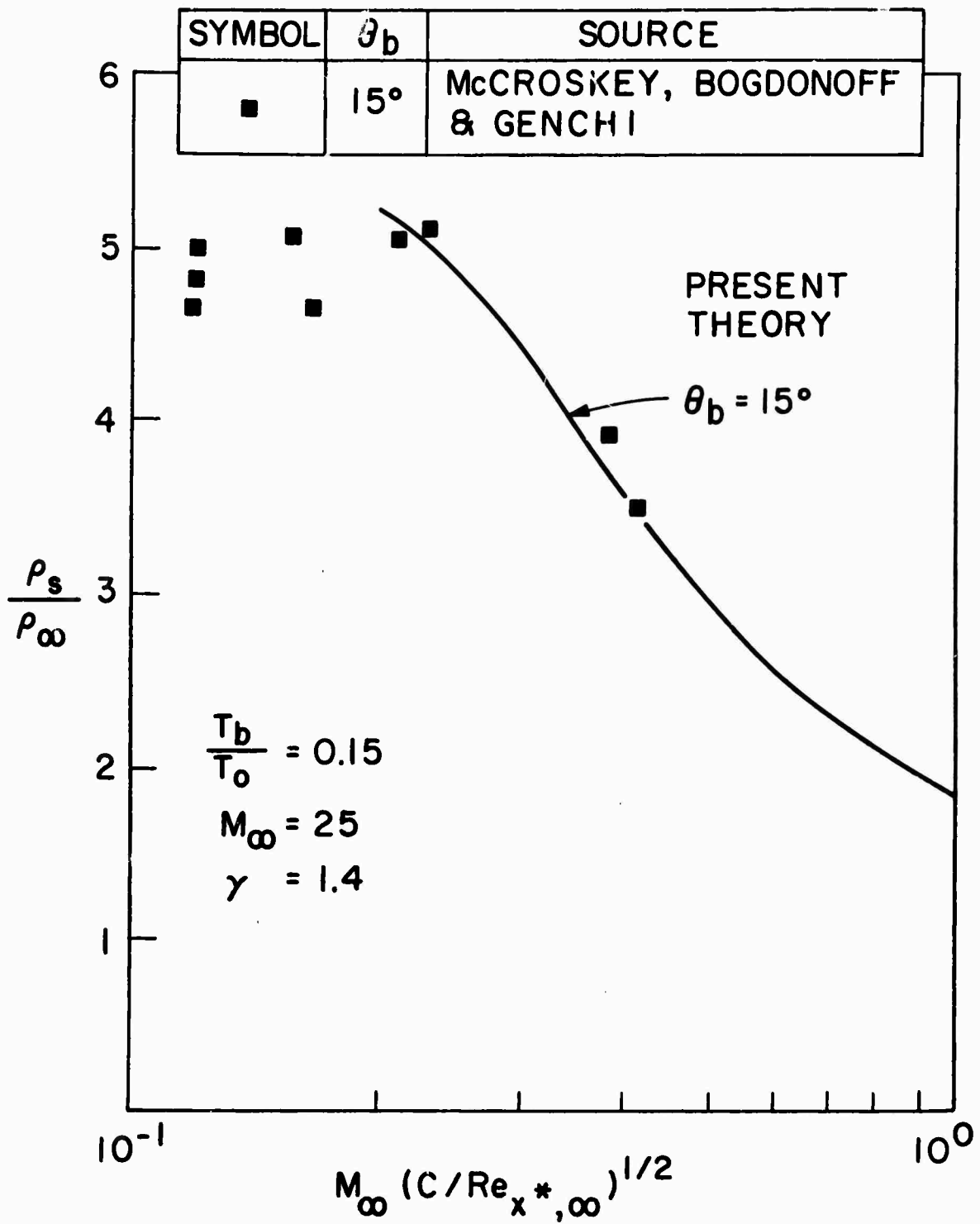


Fig. 5 Density ratio across the shock structure for a wedge

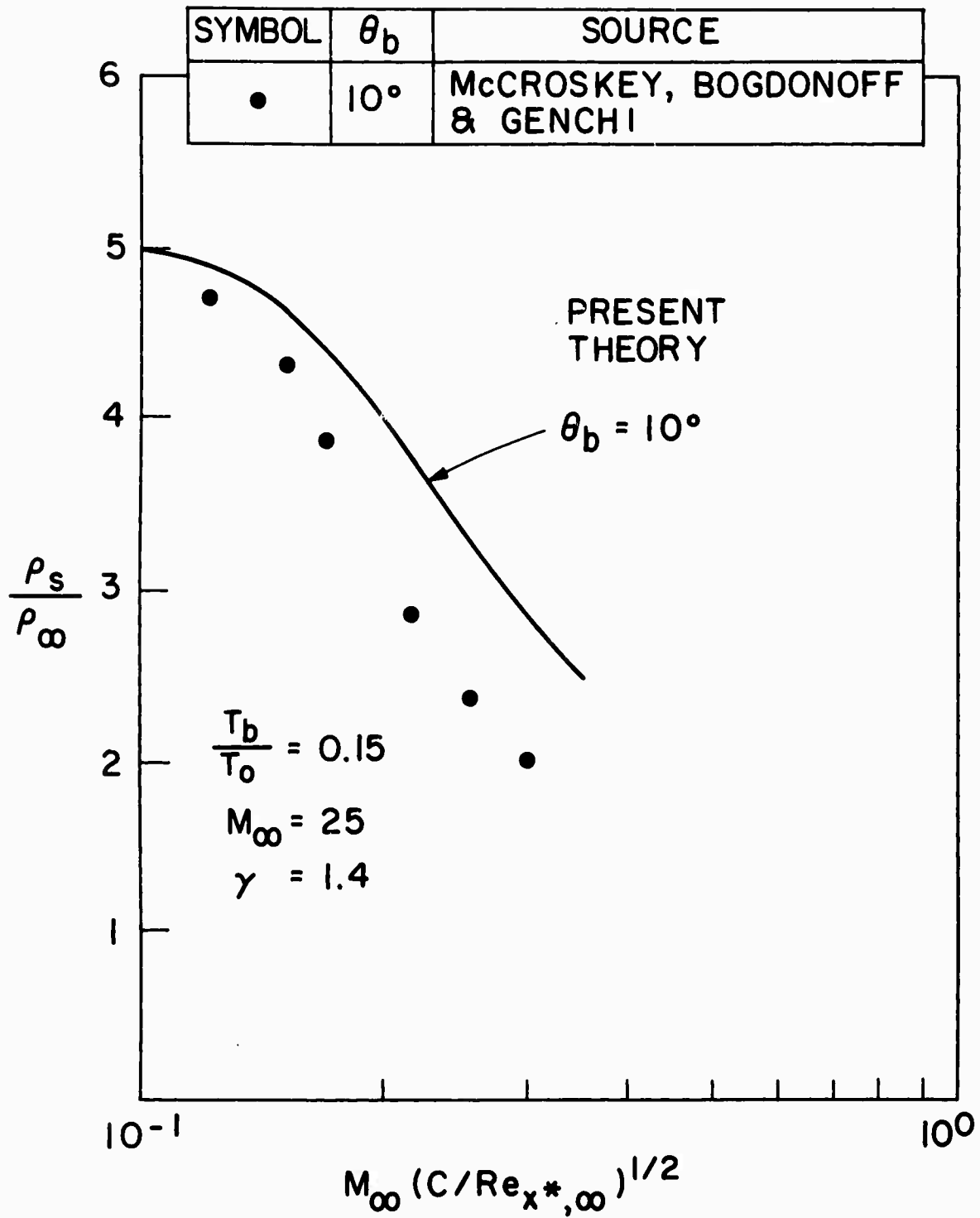


Fig. 6 Density ratio across the shock structure for a cone

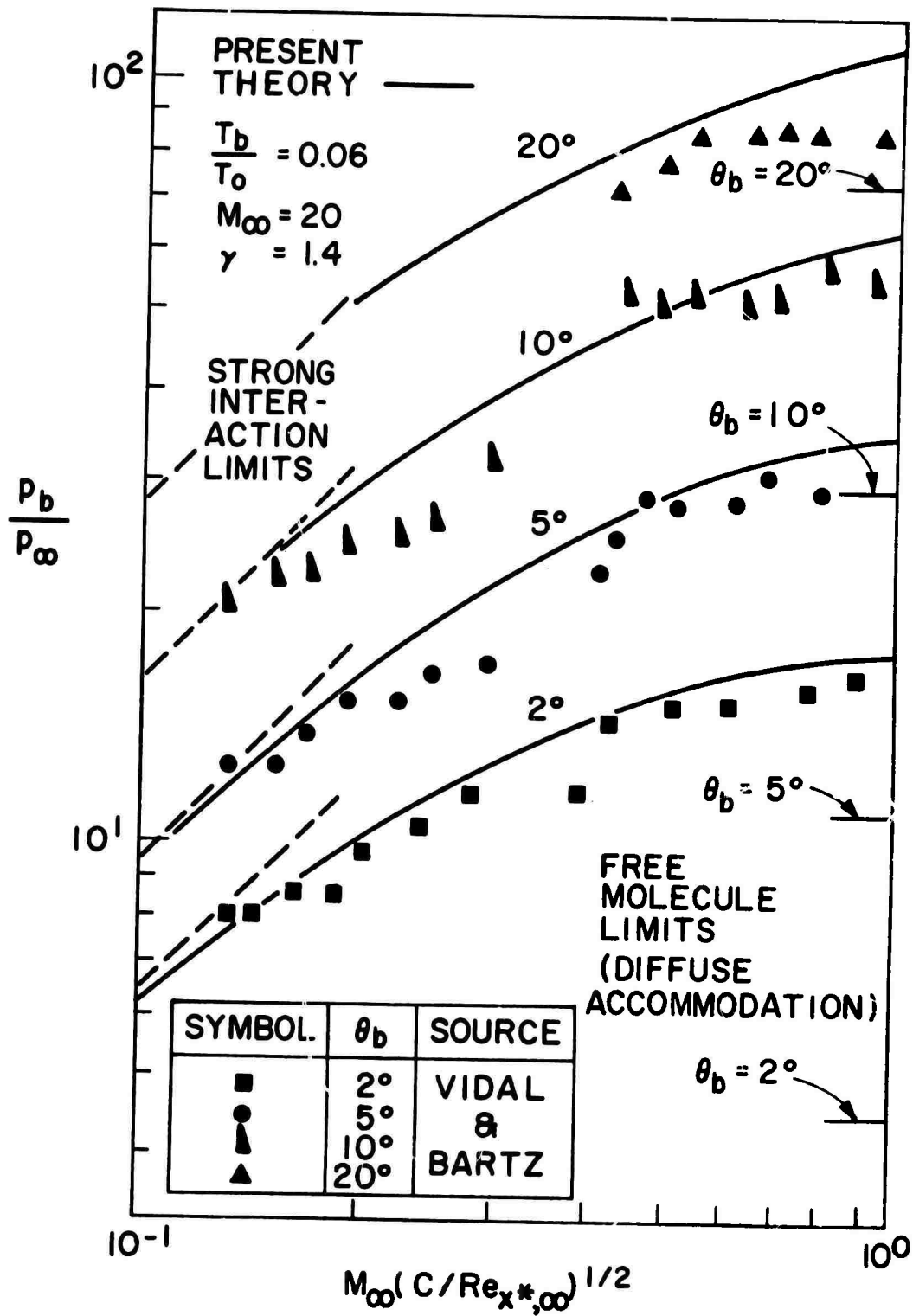


Fig. 7 Wall pressure on wedges

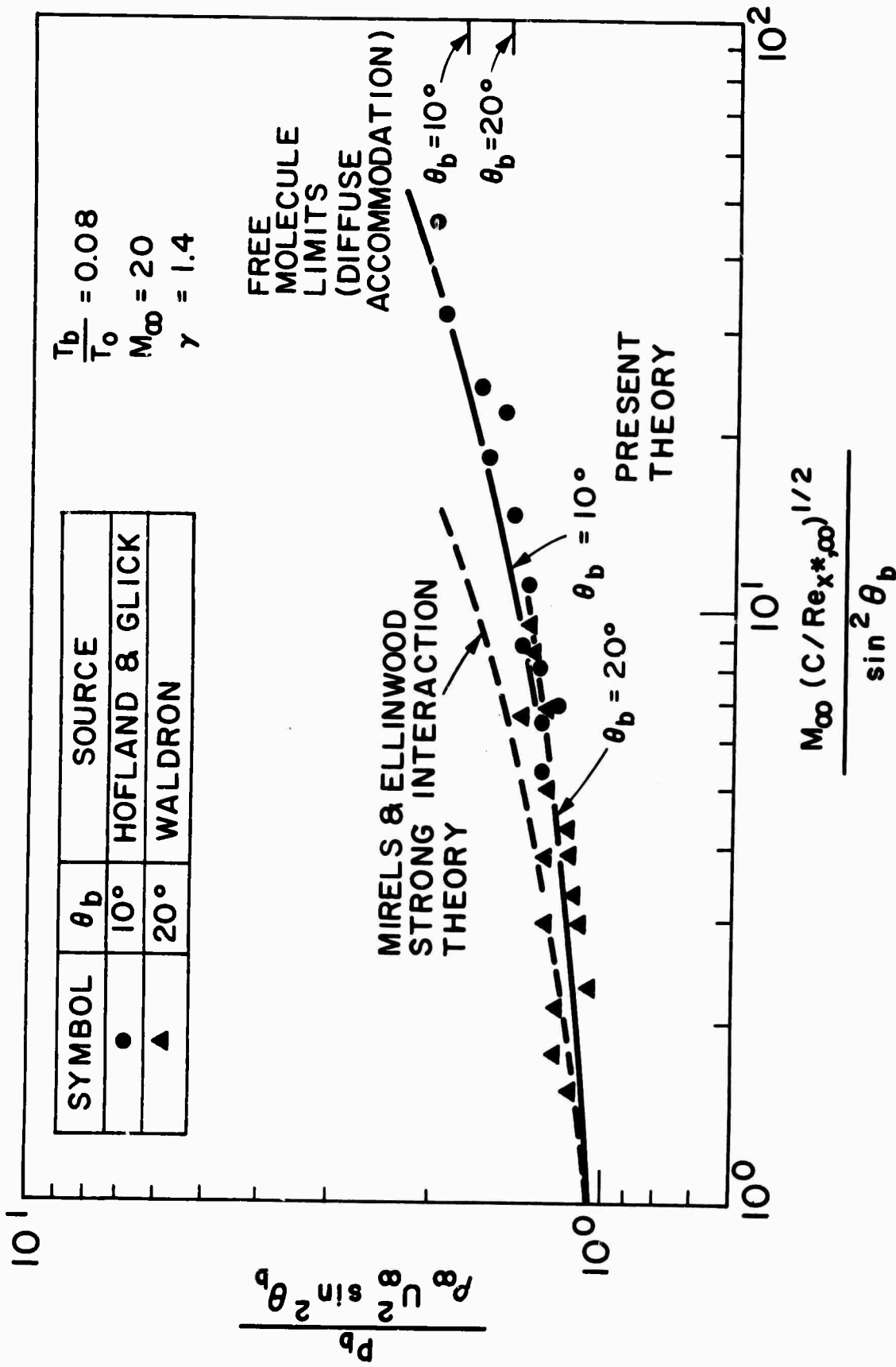


Fig. 8 Wall pressure on cones

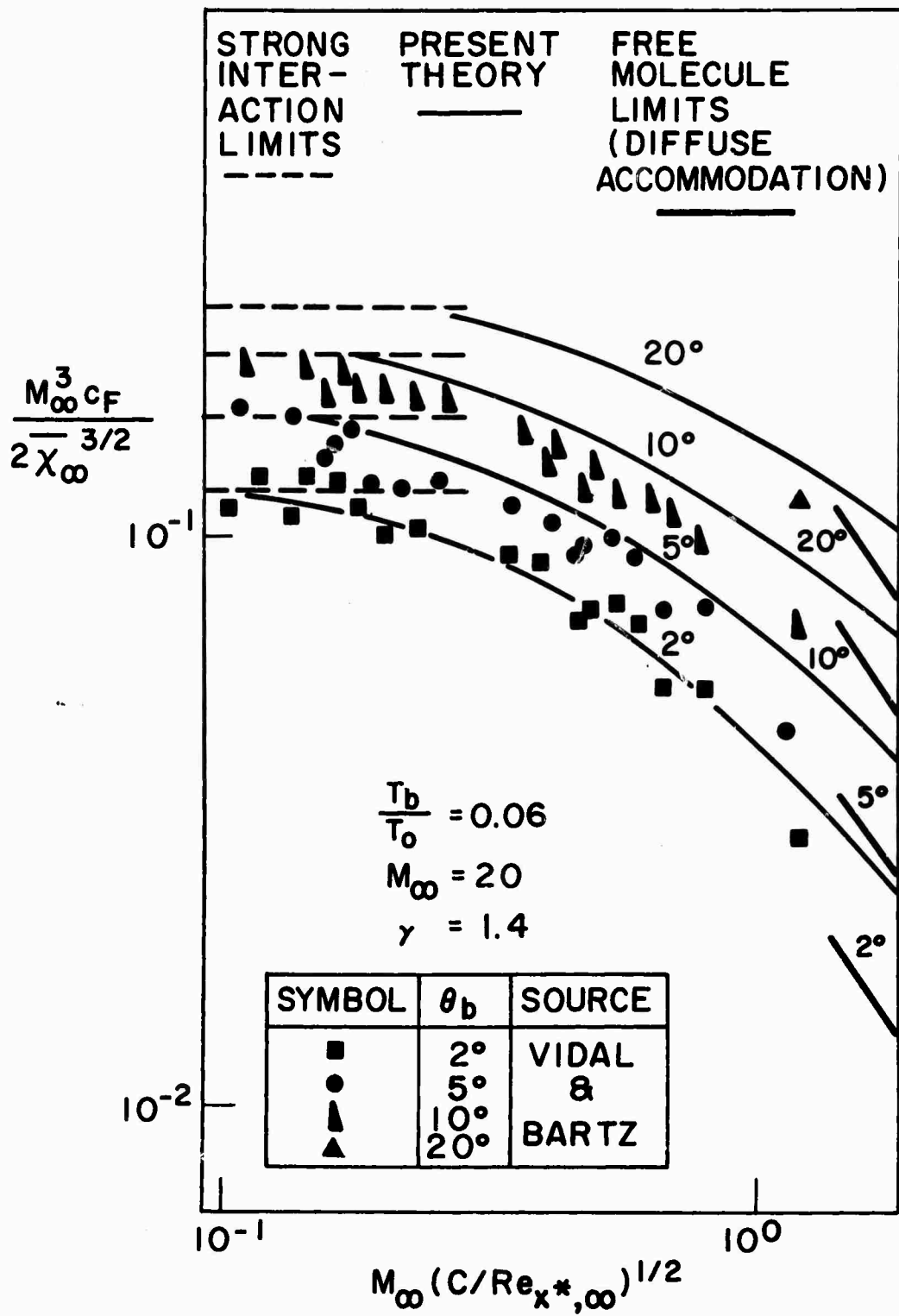


Fig. 9 Skin friction on wedges

HD

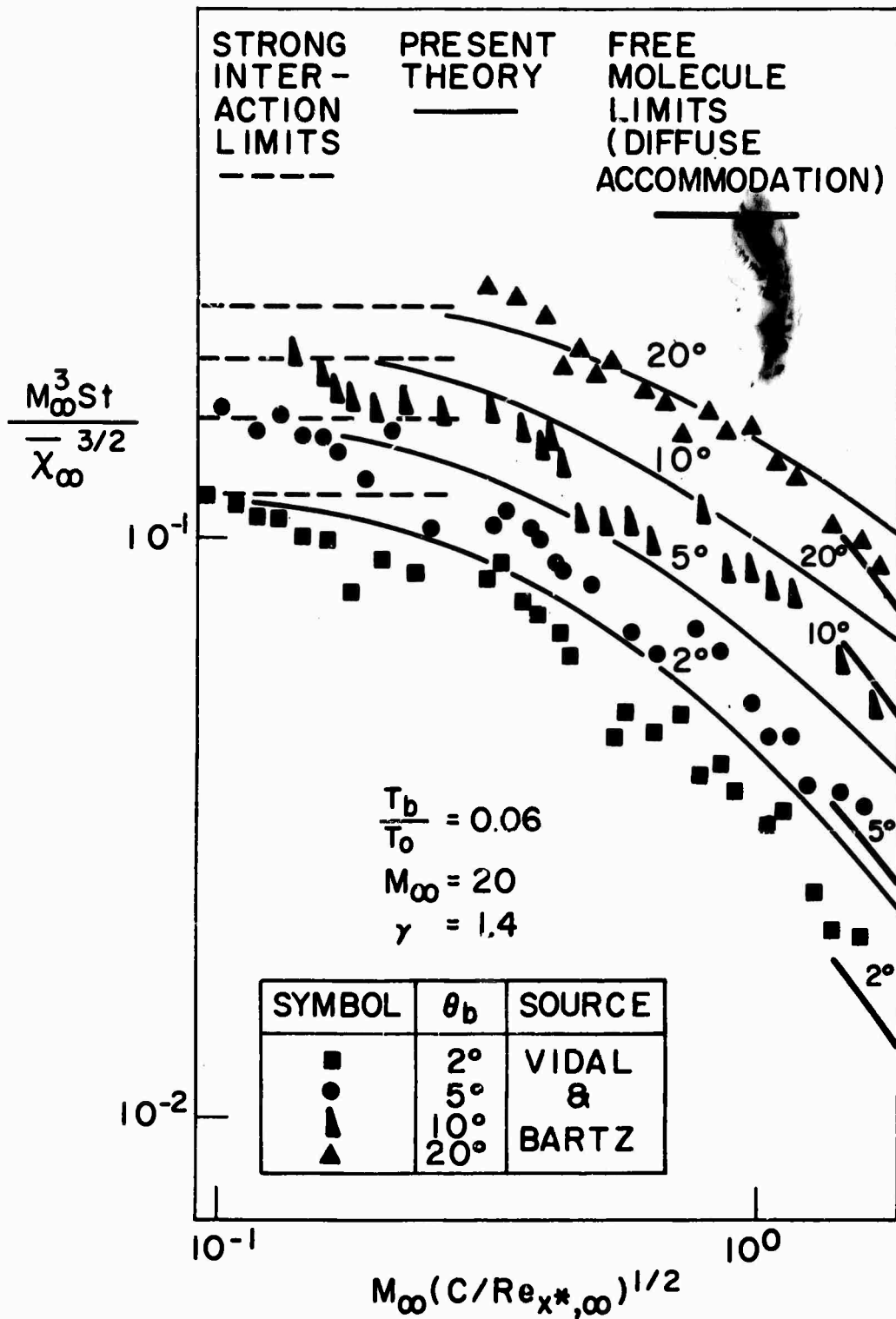


Fig. 10 Heat transfer rate on wedges

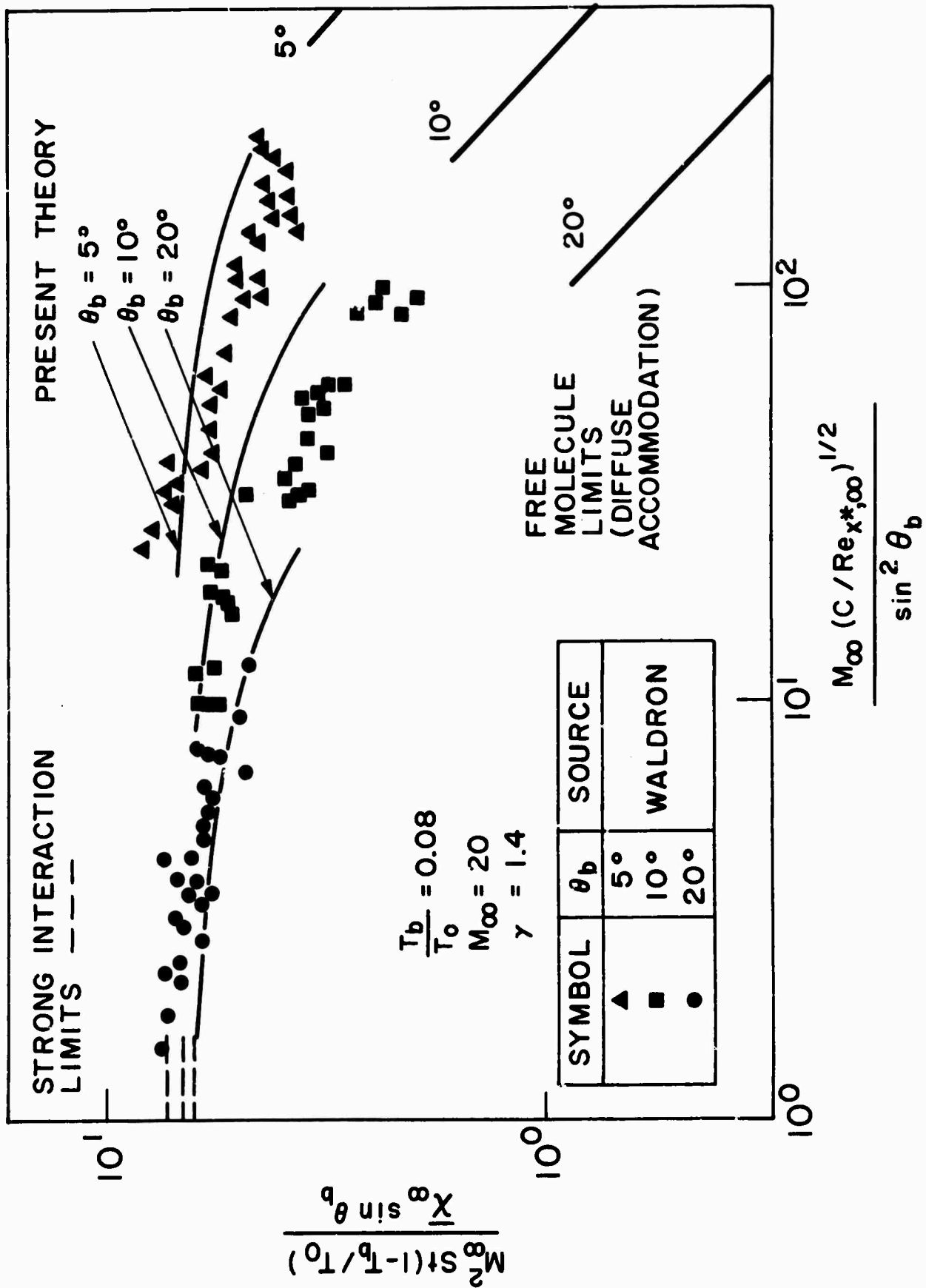


Fig. 11 Heat transfer rate on cones